AD___________________

Award Number: W81XWH-04-1-0594

TITLE: Pre-Clinical and Clinical Evaluation of High Resolution, Mobile Gamma Camera and Positron Imaging Devices

PRINCIPAL INVESTIGATOR: David R. Gilland, Ph.D.

CONTRACTING ORGANIZATION: University of Florida
Gainesville, FL 32611

REPORT DATE: June 2006

TYPE OF REPORT: Annual

PREPARED FOR: U.S. Army Medical Research and Materiel Command
Fort Detrick, Maryland 21702-5012

DISTRIBUTION STATEMENT: Approved for Public Release;
Distribution Unlimited

REPORT DOCUMENTATION PAGE

Form Approved
OMB No. 0704-0188

1. REPORT DATE *(DD-MM-YYYY)*
01-06-2006

2. REPORT TYPE
Annual

3. DATES COVERED *(From - To)*
13 May 2005 - 13 May 2006

4. TITLE AND SUBTITLE
Pre-clinical and Clinical Evaluation of High Resolution, Mobile Gamma Camera and Positron Imaging Devices

5a. CONTRACT NUMBER

5b. GRANT NUMBER
W81XWH-04-1-0594

5c. PROGRAM ELEMENT NUMBER

6. AUTHOR(S)
David R. Gilland, Ph.D.

E-Mail: gilland@ufl.edu

5d. PROJECT NUMBER

5e. TASK NUMBER

5f. WORK UNIT NUMBER

7. PERFORMING ORGANIZATION NAME(S) AND ADDRESS(ES)

University of Florida
Gainesville, FL 32611

8. PERFORMING ORGANIZATION REPORT NUMBER

9. SPONSORING / MONITORING AGENCY NAME(S) AND ADDRESS(ES)
U.S. Army Medical Research and Materiel Command
Fort Detrick, Maryland 21702-5012

10. SPONSOR/MONITOR'S ACRONYM(S)

11. SPONSOR/MONITOR'S REPORT NUMBER(S)

12. DISTRIBUTION / AVAILABILITY STATEMENT
Approved for Public Release; Distribution Unlimited

13. SUPPLEMENTARY NOTES

14. ABSTRACT:
The objective of this project is to design, build and evaluate a compact and mobile gamma and positron imaging camera. This imaging device has several advantages over conventional systems: (1) greater flexibility in positioning with respect to the target organ for improved spatial resolution and sensitivity, (2) the ability to image patients who cannot be transported to a radiology suite, (3) the potential for improved cost effectiveness for organ-specific imaging tasks compared with larger, general purpose imaging systems. Simulation studies have demonstrated the potential image quality that can be produced with this device operating in either dual gamma, coincidence mode or single gamma mode. The construction of the system gantry has been completed and the mechanical testing is nearly completed. The gantry has demonstrated the ability to position the detectors, with respect to the patient on an intensive care unit bed, as the design specified. Detector design and fabrication is nearly completed. Images have been obtained from a small field of view, prototype detector, which demonstrated satisfactory performance. Fast data acquisition electronics for high count rate capability have been built and tested.

15. SUBJECT TERMS
PET, SPECT, Cardiac Imaging, Detectors

16. SECURITY CLASSIFICATION OF:			17. LIMITATION OF ABSTRACT	18. NUMBER OF PAGES	19a. NAME OF RESPONSIBLE PERSON
a. REPORT	b. ABSTRACT	c. THIS PAGE			USAMRMC
U	U	U	UU	10	19b. TELEPHONE NUMBER *(include area code)*

Standard Form 298 (Rev. 8-98)
Prescribed by ANSI Std. Z39.18

Table of Contents

INTRODUCTION

The objective of this project is to design, build and evaluate a compact and mobile camera for gamma and positron imaging. This imaging device has several advantages over conventional systems: (1) improved spatial resolution and sensitivity due to greater flexibility in positioning with respect to the target organ, (2) the ability to image patients who cannot be transported to a radiology suite, (3) the potential for improved cost effectiveness for organ-specific imaging tasks compared with larger, general purpose imaging systems. Once built, the performance of this imager will be evaluated using physical phantoms.

BODY

Simulation Studies

In our last quarterly report, we describe our investigation into the use of an alternative simulation program; namely, the “SIMIND” simulation program for SPECT developed at Lund University, Sweden [1]. This program is much more efficient than the “GATE” simulation program [2], which we have used throughout this project. However, we have found that the SIMIND program lacks the capability of accurately simulating the effects of collimator septal penetration, and this is a key effect to study for the application of SPECT imaging of 511 keV photons.

We have begun investigating a method for efficiently incorporating realistic penetration effects into the SIMIND simulation output. In doing so, we hope to achieve the efficiency of the SIMIND approach but with the accuracy of the GATE approach in terms of modeling collimator penetration. The method relies on computing a “septal penetration function” (SPF) that can be used in a filtering operation applied to the SIMIND output. The SPF is defined to be equal to the modulation transfer function of the GATE output divided by the modulation transfer function of the SIMIND output.

Our initial tests of this approach (reported in the last quarterly report) included images of a point source in air and revealed the distance-dependent nature of the SPF: the shape of the SPF changes with distance from the detector. In light of this finding, we have investigated an approach in which the SPF is computed as a function of distance from the detector, and this distance-dependent function is stored in a look-up table. The method for incorporating the distance-dependent SPF into the SIMIND output involves computing the projection data from one plane of the source object at a time. The source planes are parallel to the detector plane, and based on the distance of the source plane to the detector, the appropriate distance-dependent SPF is applied during the projection calculation. We have computed the SPF look-up table in increments of 1 cm distance to the detector.

Figure 1 illustrates this approach. Figure 1A shows the GATE projection image of a simulated heart phantom. Figure 1B shows the SIMIND projection image of the same phantom. Note the lack of detected events in regions outside of the heart region due to the absence of collimator penetration effects. Figure 1C shows the SIMIND image from Fig. 1B after application of the SPF approach. The similarity of the profiles of the images in Figs. 1A and 1C indicate the effectiveness of this approach. In this case, we assumed the effects of attenuation and scatter were negligible. We now plan to investigate the accuracy of this approach under the more realistic conditions in which attenuation and scatter effects are present.

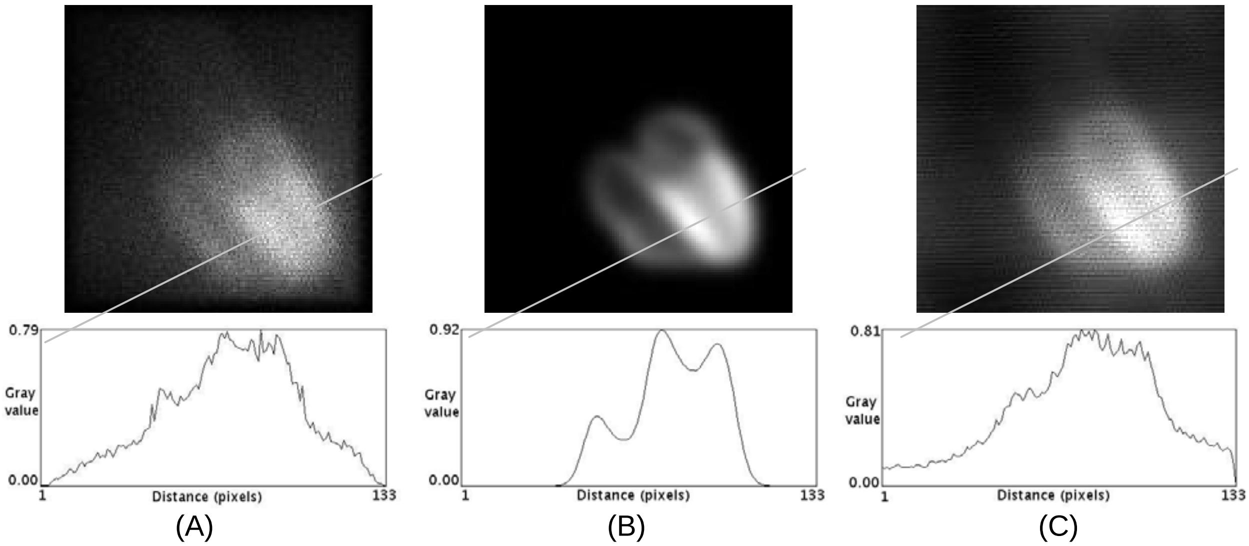

Fig. 1. Projection images of simulated heart phantom and intensity profiles through images. The location of profiles within images is indicated by solid lines. (A) Gate result, (B) Simind result, (C) Simind result with penetration modeling by SPF approach.

Gantry Design, Construction and Evaluation

The design and fabrication of the gantry has been completed, and the testing of the gantry is in final stages at UF. The electro-mechanical gantry will allow the detectors to be transported within a hospital and will be capable of precise positioning with respect to the patient.

In tests with a volunteer lying supine on an intensive care unit bed, the gantry was able to position mock detectors in anterior/posterior opposing, lateral opposing, and anterior "L" orientations (Fig. 2). The base of the gantry has a low profile that allows the base to travel below the support railing of the bed to provide a stable foundation. The horizontal and vertical positions of the two gantry arms are digitally encoded and read-out onto LED displays on the gantry panel (not shown in Fig. 2). Additional position sensors—electronic protractors that will measure the angle of the detectors on the mounting axles—have been purchased and will be mounted to the mock detectors for testing and to the actual detectors once they have been fabricated.

A remaining test of the gantry involves including mock collimators on the mock detectors, which will increase the detector thickness by approximately 5 cm. We anticipate that this added thickness will not impede detector positioning.

Fig. 2: Photographs of system gantry with mock detectors positioned in anterior/posterior opposing (left), lateral opposing (center), and anterior "L" orientations.

Detector Design, Construction and Evaluation

A prototype detector for the mobile imaging system has been designed and fabricated and is currently undergoing experimental evaluation. A detailed description of this effort is included in Appendix, which is the extended abstract that was recently submitted to the 2006 IEEE Nuclear Science Symposium and Medical Imaging Conference. This work was primarily carried out at Thomas Jefferson National Accelerator Facility, which is a subcontractor on this grant. A summary description is included here.

The detector consists of a pixilated NaI scintillator with individual scintillator pixels that are 5 mm x 5 mm in cross-section and 12.5 mm thick. The total crystal area is approximately 25 cm x 25 cm (Fig. 3, right). The scintillator is optically coupled to an array of position-sensitive photomultiplier tubes (PSPMT). The 4x4 array of PSPMT's (Burle, model 850012-800) are highly compact, particularly in thickness, which makes them ideal for a compact detector design (Fig. 3, left).

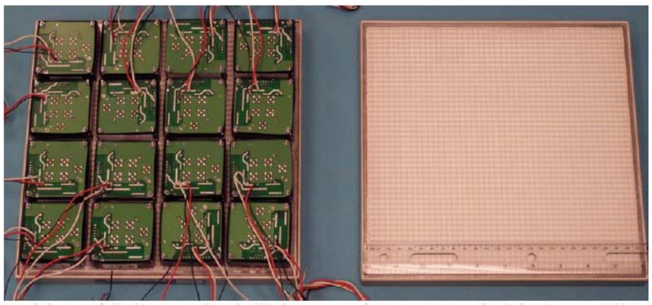

Fig. 3: Left: bottom view of detector showing photomultiplier tube array, Right: view of pixilated NaI scintillator

The output of the PSPMT's is handled by high-speed data acquisition (DAQ) electronics for high detector count rate capability. Our initial plans to use a VME-based multi-channel DAQ system encountered a major problem by our inability to pass a rather low rate event limit of only 25-30kHz in practical implementations of our VME DAQ prototype systems. We, therefore, decided to aggressively pursue a completely different method by building our own fast field-programmable gate array (FPGA) DAQ system. To achieve high rate capability, each detector head is connected to a separate, 64 channel FPGA DAQ card which is in turn read via a USB2 link to a hard drive of a separate data acquisition PC. Two data acquisition PCs, one for each detector, send the collected data files for processing to an "event builder" computer where time-stamped data files from each detector are processed and fused into one coincident file or treated separately when used in a single gamma mode. During the coincident file event building phase, the time-stamped events corresponding to two coincident 511 keV quanta are processed and put into a summary file. The summary file lists the calculated x,y gamma event positions and the gamma energies for the two gammas (one from each detector), plus a single time stamp for the coincidence event.

Initial tests of detector performance were carried out using a Na-22 point source. Figure 4 shows an example of a raw flood image from a fully illuminated detector head after first-order gain uniformity correction (by adjusting high voltage biases of individual PSPMTs). Good pixel separation over the whole field-of-view is observed. Response non-uniformities are still evident due to the remaining gain differences and dead regions between individual PSPMTs. This detector operates with over 100 kHz coincidence trigger rate. The measured energy resolution for selected pixels ranged from 15 to 20%.

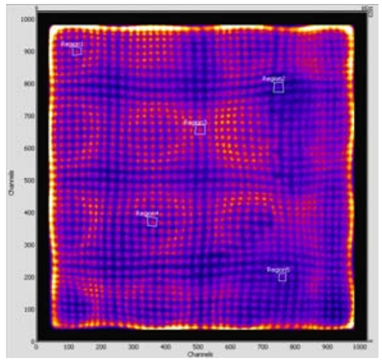

Fig. 4: Flood image for prototype detector.

In the week preceding the submission of this report, a second detector was built, and tests were performed on the pair of detectors operating in coincidence mode. A Na-22 point source was placed between the two opposing detectors (closer to the left detector), which were 25 cm apart. Figure 5A and 5B show the raw coincidence images for the left and right detectors, respectively. Spatial separation of the detector pixels is evident in this coincidence data. Figure 5C shows the detected energy spectrum from these measurements. An average energy resolution across the field-of-view of approximately 20% was observed.

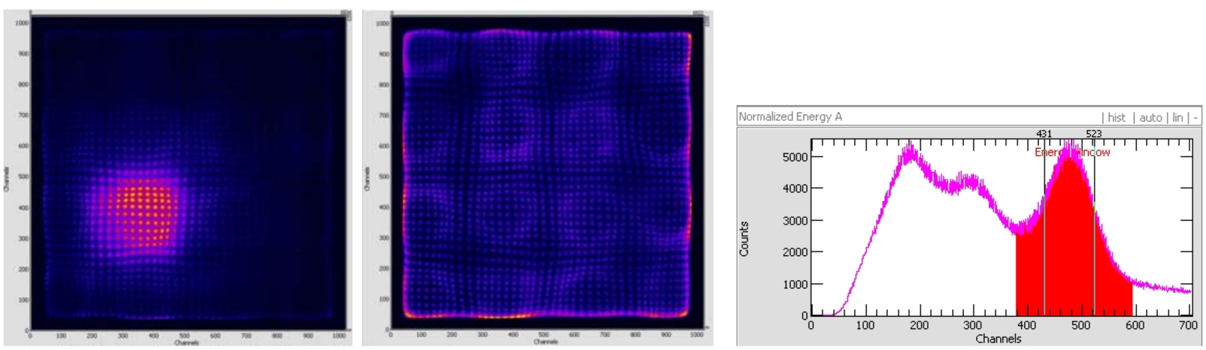

(A) (B) (C)

Fig. 5: (A,B) Coincidence images and (C) measured energy spectrum

Remaining tests of the prototype detector include sensitivity measurements for the 12.5 mm thick scintillator crystal. We are also in communication with the scintillator manufacturer (Saint Gobain Crystals) to investigate the possibly of manufacturing and evaluating a 25.4 mm thick scintillator. The thicker scintillator will offer improved detector efficiency.

KEY RESEARCH ACCOMPLISHMENTS

I. SIMULATION STUDIES

- Development of software simulation tools
    - o Novel method for efficiently incorporating collimator effects into SPECT simulation program
    - o Validation of collimator simulation using cardiac phantoms

II. GANTRY DESIGN AND CONSTRUCTION

- Completed gantry construction and delivery to UF

- Evaluation of gantry mechanical performance using mock detectors and an intensive care unit bed.

III. DETECTOR DESIGN AND CONSTRUCTION

- Development of new FPGA-based data acquisition electronics for high count rate capability
- Fabrication of prototype detector consisting of pixilated NaI scintillator (25 cm x 25 cm) and 4x4 array of position sensitive photomultiplier tubes.
- Initial testing with Na-22 flood field showed satisfactory pixel separation and energy resolution

REPORTABLE OUTCOMES (since last annual report)

Conference Proceedings:

1. Majewski S, Gunning W, Hammond R, Kross B, Smith M, Popov V, Proffitt J, Weisenberger A, Wojcik R, and Gilland D. Development and Evaluation of Detector Heads and Readout for a Mobile Cardiac Imager System. Submitted to: 2006 IEEE Nuclear Science Symposium Conference Record, May 2006.

Presentations:

1. Dingley J, Tipnis UJ, Gilland DR. Cardiac 511 keV SPECT simulation with a compact detector design. Presented at the IEEE 2005 Nuclear Science Symposium and Medical Imaging Conference, October 26-29, 2005, Fajardo, Puerto Rico.

CONCLUSIONS

We have made substantial progress in three key areas. First, we have developed simulation tools that allow us to investigate the application of SPECT imaging of 511 keV gamma photons in the context of this mobile camera. Second, we have built and tested the gantry that will support the detectors and provide the mechanical capability for detector positioning and overall system transport. Third, we have built a prototype detector with associated electronics and have evaluated the performance with basic point source measurements.

The medical benefits that this device will bring promise to be substantial, not only for the military health care system but also for health care of the general population. This device will be capable of delivering critical diagnostic imaging (PET and SPECT) to patients who otherwise cannot benefit from these technologies. Also, this device potentially can be a cost effective alternative to conventional PET systems for cardiac imaging. Finally, with the accelerated growth in the development of imaging agents for PET and SPECT, there will be a greater need for novel and dedicated imaging devices, such as the device developed in this project.

REFERENCES

1. Ljungberg M. The SIMIND Monte Carlo program. In “Monte Carlo Calculation in Nuclear Medicine: Applications in Diagnostic Imaging”, Ljungberg M, Strand S-E, King MA, eds.), pp. 145-163. IOP Publishing, Bristol and Philadelphia.
2. Website: http://www-lphe.epfl.ch/~PET/research/gate

APPENDICES

See attachment for Appendix 1.

Development and Evaluation of Detector Heads and Readout for a Mobile Cardiac Imager System

S. Majewski, W. Gunning, R. Hammond, B. Kross, M. Smith, V. Popov, J. Proffitt, A. Weisenberger, R. Wojcik, and D. Gilland

Introduction

The University of Florida mobile cardiac imager under development for heart patient's imaging in an intensive care/emergency room environment will use two detector heads, each with active field of view of about 25 cm x 25 cm and 5mm resolution, mounted to a two-arm gantry with the capability of positioning the two opposing detectors in the anterior/posterior and lateral patient orientations in a limited angle PET acquisition. Each detector head is designed to operate in a wide energy range from 60 keV to 511 keV. In addition to a standard PET imaging mode with two heads operating in coincidence, application of a 511 keV capable collimator is also planned to enable single gamma imaging at this energy. In this mode, the detectors will orbit the patient anterior 180 degrees.

Results of system development and initial performance tests of detector heads with the dedicated novel data acquisition system are presented in this paper.

The basic philosophy behind the design was to use a modular structure allowing parallel data recording and processing to achieve high system rate capability. Three major novel technical features of the system are: (1) use of a novel in-house developed high rate FPGA based DAQ ADC system, (2) multi-modular structure of the imager heads with position interpolation between the individual modules, and (3) implementation of large (25cmx 25cm coverage) arrays of very compact Burle 85002-800 microchannel plate-based PMTs.

Equipment and methods

The basic PMT detector module is based on Burle 85002-800 four pad microchannel plate-based position sensitive photomultiplier with high-rate four analog outputs. Sixteen PSPMT units are arranged in a spaced (1cm gap distance) 4x4 array to form each detector head with 25cmx25cm FOV (figure 1). The rationale for this particular solution was high performance in a compact mobile package, but also economy. A total of 64 analog outputs are therefore read per detector head and the total number of ADC channels for the whole system is 128. The fast pulse per detector head is formed from summing all 64 pad and producing corresponding fast constant fraction discriminator trigger pulse for two-head coincidence requirement or single gamma imaging mode trigger. (Details of the on-board electronics will be presented at an accompanying technical paper at this conference.)

A special interconnect board collects pad signals from individual PMTs for transfer via cables to the DAQ system, and distributes individually adjusted HVs to each PMT module. The individual HV PMT bias voltages are adjusted to assure that all PMT modules in the detector head have similar signal response to the same initial energy deposit (511 keV), with the exception of "dead" regions between PSPMTs, where the signal drops down to about 55%, when appropriate light guides are implemented. Each scintillation array (made by Saint Gobain Crystals and Detectors) of 5x5x12.5-25 mm NaI(Tl) pixels spaced at 5.5mm covers an area of about 25x25cm. The pixels are optically separated by special white reflective/ diffusive epoxy material.

To assure good optical coupling to PMTs of scintillator pixels placed in front of the dead regions between the sparsely placed individual PMTs, an additional optical window-spacer was added between the encapsulated behind a 5mm glass window scintillation array and PMTs. This extra window is made of a high quality 20 mm thick UV acrylic plate. To guarantee long-term optical coupling stability, only dry optical couplings were used between both windows and PMTs.

Our initial plans to use a VME-based multi-channel DAQ system encountered a major problem by our inability to pass a rather low rate event limit of only about 25-30kHz in practical implementations of our VME DAQ prototype systems. While the attained limit is not necessarily indicative of the intrinsic limit of the VME-based systems we decided to abandon the original approach and to aggressively pursue a completely different method by building our own fast FPGA DAQ system. We succeeded and all the results presented in this report are obtained with this new readout.

To achieve high rate capability, each detector head is connected to a separate 64ch FPGA DAQ card which is in turn read via a USB2 link to a hard drive of a separate data acquisition PC (figure 2). (A separate paper at this conference will describe the FPGA DAQ system development and give details of its parameters and performance.)

Two data acquisition PCs, each used for one detector head, send the collected data files for processing to a next level "event builder" computer where time-stamped data files collected separately for each detector head can be processed and fused into one coincident file or treated separately when used in a single gamma mode. During the coincident file event building phase, recorded and time-stamped events corresponding to two coincident 511 keV quanta from both detector heads are processed and put into a summary file, listing final calculated x and y gamma event positions and gamma ray energies for the two gammas from both detector heads, plus an event time stamp for each acquired coincident event, with ~5ns time accuracy.

FPGA ADC data acquisition is controlled by distributed Java-based software. Java-based server application sits on each of the acquisition computers and directly controls one FPGA ADC board through a USB2 connection. The USB driver for the FPGA board is directly accessed by C++ code; the JNI (Java Native Interface) is used to allow Java indirect control of the USB driver. The server application on each of these machines is controlled by a remote client Java-based application on the control event builder computer that coordinates the collective acquisition, transfer, and processing of data. The client application is connected to each of the four server applications through a dedicated gigabit Ethernet network. After data is acquired and written to disk on the acquisition computers, the server application transfers data to the remote client computer. Finally, the client application sorts through data from coincident detectors, matches events by time stamp, and sends data for reconstruction.

A Kmax8 based software analysis program was implemented to calibrate and characterize the two detector head system. Kmax8 is written in Java and is therefore compatible with the FPGA ADC control software. The software analysis program reads data written to disk by the acquisition software in order to display raw images, implement calibrations and corrections, and provide tools to characterize the two detector head system performances. A special position algorithm uses digitized raw pad signals from all 64 pads of sixteen PMTs to obtain raw gamma event positions. Calibration routines are then employed to calculate response-corrected true positions and energies of gamma events.

A ^{22}Na point source was used during initial laboratory tests. Few examples of initially obtained results are presented in the attached below figures 3-4.

Summary and highlights of results (May 2006)

The developed modular design cardiac imager can operate with over 100 kHz coincidence trigger rate and achieves uniform detection efficiency across the 25x25 cm FOV, including dead regions between PMTs where signal decreases to no less than about 55% relative to the on-PMT signal value. Initial timing resolution of about 5ns FWHM was achieved for a single detector head (against fast trigger detector).

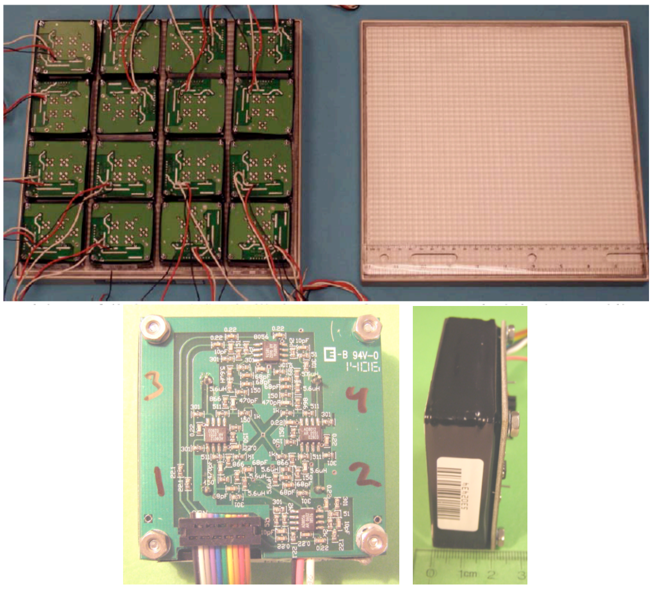

Figure 1: At top are shown PMTs as arranged in a slightly spaced configuration to cover the 25cmx25cm FOV of the 5mm pixel NaI(Tl) scintillation array, which is also pictured separately at top right. In the two bottom pictures a single PMT with attached amplifier board is shown in two views. Total thickness of the very compact package PMT+card+connectors is less than 30 mm.

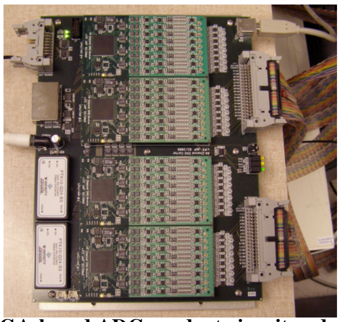

Figure 2: Fast FPGA-based ADC readout circuitry developed by James Proffitt at Jefferson Lab for the readout of positron imagers. Two boards with four 16ch ADC cards each, like the one shown here, are used to read a pair of cardiac detector heads.

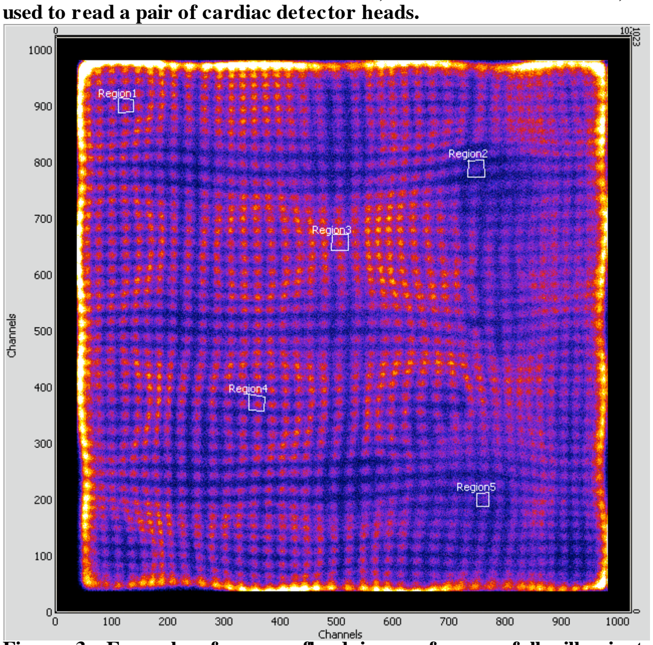

Figure 3: Example of a raw flood image from a fully illuminated detector head (with a ^{22}Na source) after first-order gain uniformity correction (by adjusting HV biases of individual PMTs). Good pixel separation over the whole field-of-view is observed. Response non-uniformities are still evident due to remaining gain differences, dead regions between individual photomultipliers, and low granularity (~1 inch) of the PMT pad readout.

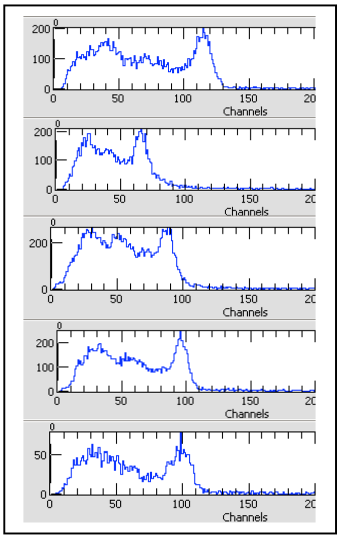

Figure 4: Examples of ^{22}Na energy spectra obtained from selected characteristic five NaI(Tl) pixels (corresponding ROIs are shown in the raw image in figure 3). All pixels show good energy resolution of about 15-20% @ 511 keV photopeak confirming proper operation of the detector across all regions of the active surface. The range of amplitudes of about factor ~2 is observed after first-order adjustment of response uniformity.